JOURNAL OF
AGRICULTURAL AND
FOOD CHEMISTRY

Modeling the Formation of Some Polycyclic Aromatic Hydrocarbons During the Roasting of *Arabica* Coffee Samples

JUSTIN KOFFI HOUESSOU,[†,‡] DANIEL GOUJOT,[§,||,⊥] BERTRAND HEYD,[§,||,⊥] AND
VALERIE CAMEL*,[†,‡]

AgroParisTech and INRA, UMR214 Ingénierie Analytique Pour la Qualité des Aliments,
F-75005 Paris, AgroParisTech and INRA, UMR1145 Génie Industriel Alimentaire, F-91300 Massy,
and CEMAGREF, UMR1145 Génie Industriel Alimentaire, F-91300 Massy, France

Roasting is a critical process in coffee production, as it enables the development of flavor and aroma. At the same time, roasting may lead to the formation of nondesirable compounds, such as polycyclic aromatic hydrocarbons (PAHs). In this study, *Arabica* green coffee beans from Cuba were roasted under controlled conditions to monitor PAH formation during the roasting process. Roasting was performed in a pilot-spouted bed roaster, with the inlet air temperature varying from 180 to 260 °C, for roasting conditions ranging from 5 to 20 min. Several PAHs were determined in both roasted coffee samples and green coffee samples. Different models were tested, with more or less assumptions on the chemical phenomena, with a view to predict the system global behavior. Two kinds of models were used and compared: kinetic models (based on Arrhenius law) and statistical models (neural networks). The numbers of parameters to adjust differed for the tested models, varying from three to nine for the kinetic models and from five to 13 for the neural networks. Interesting results are presented, with satisfactory correlations between experimental and predicted concentrations for some PAHs, such as pyrene, benz[*a*]anthracene, chrysene, and anthracene.

KEYWORDS: Coffee; kinetic model; neural network; polycyclic aromatic hydrocarbons; roasting

INTRODUCTION

The presence of polycyclic aromatic hydrocarbons (PAHs) in coffee samples was first reported by Kuratsune and Hueper (*1*) and Fritz (*2*). Since then, a few publications have dealt with the analysis of such contaminants in coffees (*3−6*). However, studies differ by the type of coffee studied (milled coffees, instant coffee, or coffee brew), the sample origins (Brazil, Colombia, Ethiopia, etc.), the roasting conditions (green coffee or roasted coffee under noncontrolled conditions most of the time), and the coffee brew preparation conditions, so that comparisons between them are difficult. Yet, the PAH contamination of green beans has been reported, as well as the formation or the degradation of PAHs upon roasting with possible toxic equivalents around 2 μg kg^{-1} (*7*). There are several maximum limits (ranging from 1.0 to 10.0 μg kg^{-1}) in

the European Union for benzo[*a*]pyrene in different kinds of food, but none has yet been proposed for coffee (*8*).

PAHs in coffee samples may come either from a contamination of green coffee beans (such as contamination during the drying step) or from an endogenous formation in the coffee beans during the roasting process. Indeed, roasting is a crucial step for the production of coffee, as it enables the development of color, aroma, and flavor, which are essential for the characterization of the coffee quality. In practice, roasting conditions differ depending on the coffee quality expected and the type of roaster used. Both the temperature and the time conditions of the roasting step need to be optimized and controlled to achieve maximum aroma and flavor development.

During coffee roasting, many substances are formed due to numerous chemical reactions occurring at high temperatures that can contribute to the taste and aroma of coffee, whereas others may present harmful effects on humans such as mutagenicity, as reported (*9*). Even though PAHs are hydrophobic, their presence in coffee brew has been reported (*4, 5, 10*). As a matter of fact, despite several possible beneficial effects (*11*), coffee is still classified 2B "possibly carcinogenic to humans" by the International Agency for Research on Cancer with regard to urinary bladder, as there is limited evidence of a relationship between coffee drinking and this type of cancer (*12*).

* To whom correspondence should be addressed. Tel.: 33-1-44-08-17-25. Fax: 33-1-44-08-16-53. E-mail: valerie.camel@agroparistech.fr.
† AgroParisTech, UMR214 Ingénierie Analytique Pour la Qualité des Aliments.
‡ INRA, UMR214 Ingénierie Analytique Pour la Qualité des Aliments.
§ AgroParisTech, UMR1145 Génie Industriel Alimentaire.
|| INRA, UMR1145 Génie Industriel Alimentaire.
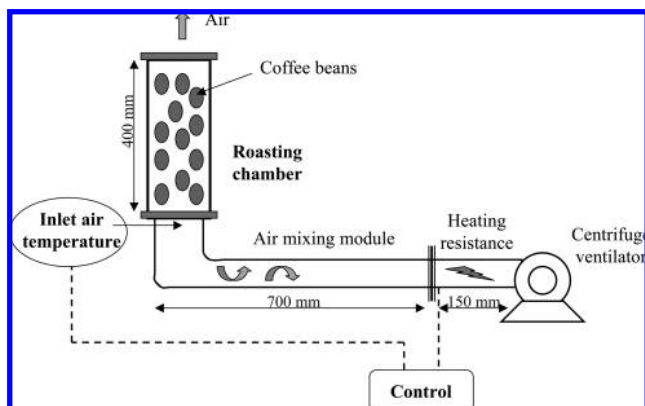⊥ CEMAGREF, UMR1145 Génie Industriel Alimentaire.

Formation of Some PAHs during Coffee Roasting

J. Agric. Food Chem., Vol. 56, No. 10, 2008   **3649**

Figure 1. Schema of the pilot-spouted bed roaster used in this study.

Table 1. Temperature Conditions Tested in This Study

inlet air temperature (°C)	outlet air temperature (°C)	mean roasting chamber temperature (°C)
180	170.4	175.2
200	188.8	194.4
220	207.1	213.5
240	225.3	232.6
250	234.4	242.1
260	243.5	251.6

Table 2. Toxic Equivalent Factors (TEF) for the 11 PAHs Determined in This Study

| compounds	abbreviation	no. of aromatic rings	IARC[a] group	TEF[b]
phenanthrene	Phen	3	3	0.001
anthracene	Anthr	3	3	0.01
fluoranthene	F	4	3	0.01
pyrene	Pyr	4	3	0.001
benz[*a*]anthracene	B[a]A	4	2A	0.1
chrysene	Chrys	4	2B	0.01
benzo[*b*]fluoranthene	B[b]F	5	2B	0.1
benzo[*k*]fluoranthene	B[k]F	5	2B	0.1
benzo[*a*]pyrene	B[a]P	5	1	1
dibenz[*a,h*]anthracene	DB[ah]A	5	2A	1
benzo[*g,h,i*]perylene	B[ghi]P	6	3[c]	0.01

[a] International Agency for Research on Cancer (IARC): Group 1, carcinogenic to humans; group 2A, probably carcinogenic to humans; group 2B, possibly carcinogenic to humans; and group 3, not classifiable as to carcinogenicity to humans. [b] From the French Food Safety Agency (AFSSA)—Saisine no. 2000-SA-005; www.afssa.fr. [c] This classification may change as this compound has been recently considered as of concern for health by the Joint Expert Committee on Food Additives (JECFA).

Chemical reactions occurring during coffee roasting are very complex, so that it is highly difficult to propose reaction schemes. In that context, modeling the behavior of PAHs during coffee roasting is quite a challenge. The aim of this paper was to investigate the formation (and possible further degradation) of several PAHs and to propose several models with a view of predicting the PAH behavior under roasting. Neural network models and kinetic models with apparent reaction schemes are presented. This could help in choosing roasting conditions that afford satisfactory sensorial coffee quality along with minimization of PAH levels, even though the sensorial aspect of coffee roasting was not studied in this work. To avoid variations in PAH concentrations related to the coffee origin as well as variation in roasting temperature related to its initial water content, only one *Arabica* sample from Cuba was considered in this study.

MATERIALS AND METHODS

Most experiments were done in triplicate, enabling mean values, median values, and relative standard deviations (RSDs) to be determined.

Reagents and Chemicals. Reagents were all used in the form purchased without additional purification or alteration. A PAH mix solution was used (Supelco, Saint-Quentin Fallavier, France) containing the 16 EPA PAHs (10 mg L^{-1} in acetonitrile) with purities above 96% as indicated: naphthalene (97.7%), acenaphthylene (99.9%), acenaphthene (99.9%), fluorene (98.6%), phenanthrene (99.9%), anthracene (99.8%), fluoranthene (98.2%), pyrene (96.6%), benz[*a*]anthracene (97.9%), chrysene (98.7%), benzo[*b*]fluoranthene (99.9%), benzo[*k*]fluoranthene (99.5%), benzo[*a*]pyrene (99.9%), dibenz[*a,h*]anthracene (99.6%), benzo[*g,h,i*]perylene (99.1%), and indeno[1,2,3-*cd*]pyrene (99.9%). High-performance liquid chromatography (HPLC)-grade solvents were used, either supplied by Carlo-Erba (Val de Reuil, France) or Prolabo (Fontenay-sous-Bois, France). Deionized water was produced with a Milli-Q system from Millipore (Saint-Quentin-en-Yvelines, France). Anhydrous sodium sulfate was supplied by Merck (for analysis grade), and potassium hydroxide (KOH) was supplied by Prolabo (Rectapur grade). Stock standard solutions were prepared by diluting the PAH solutions in an appropriate volume of tetrahydrofuran (THF) to obtain the desired concentrations in the range 5−500 μg L^{-1}. All solutions were stored at 4 °C in the dark for up to 5 weeks.

Coffee Roasting. Green coffee beans (*Arabica*) were from Cuban origin (Coffea, Le Havre, France). Green beans (100 g) were roasted in a pilot-spouted bed roaster (see **Figure 1**) (coffee beans were manually placed in the chamber before roasting). Roasting was carried out for different times (5−20 min range) and different temperatures (180−260 °C) of the inlet air. The correspondence between roaster mean chamber temperature and inlet air temperature is given in **Table 1**. This experimental domain is slightly wider

than the time/temperatures classically used in the coffee industry for a better understanding of the kinetics involved in PAH formation during roasting (*13*). The roasted beans were kept in the dark in closed polyethylene flasks, before being submitted to the sample treatment procedure recently developed and validated for the determination of the 11 PAHs reported in **Table 2** (*6*).

Extraction and Cleanup of Ground Coffee Samples. Prior to their extraction, coffee beans were ground using a coffee grinder (Prep'Line 850, power of 180 W, Seb, France). Ground coffee samples were then extracted using a pressurized liquid extraction system (ASE 100, Dionex, Voisins Le Bretonneux, France), with hexane/acetone 50:50 (v/v) under 150 °C as already detailed (*6*). The obtained extract was then concentrated to a few milliliters using a rotary evaporator and finally to dryness under a gentle stream of nitrogen, before being submitted to alkaline saponification and cyclohexane extraction as already reported (*6*). The final extract was then concentrated to a few milliliters using a rotary evaporator and finally to near 2 mL under a gentle stream of nitrogen.

The saponified extracts were cleaned-up using solid-phase extraction on disposable silica cartridges (Supelclean LC-Si, 1 g, supplied by Supelco, Saint-Quentin Fallavier, France). A Visiprep vacuum manifold system (Supelco) was used. Cartridges were conditioned with 5 mL of cyclohexane, and PAHs were eluted with 4 × 5 mL cyclohexane. After evaporation to dryness under a gentle stream of nitrogen, the dry residue was redissolved in 0.4 mL of THF before further analysis.

PAH Analysis. Extracts were analyzed using HPLC coupled to fluorimetric detection (FD). The HPLC system consisted of a Varian 9010 high-pressure gradient pump (Varian, Les Ulis, France), a Rheodyne model 7125 injection valve equipped with a 20 μL loop, a Thermo Separation Science fluorimetric detector (FL3000), and a computer. Data analysis was performed using the TurboChrom TC4 Navigator. A Supelcosil LC-PAH column (250 mm × 4.6 mm i.d., C$_{18}$ silica, 5 μm particle size, Supelco) was used, along with a precolumn (containing C$_{18}$ silica). Separation was performed using the following gradient: acetonitrile/water (60:40, v/v) for 5 min followed by a 25 min ramp to
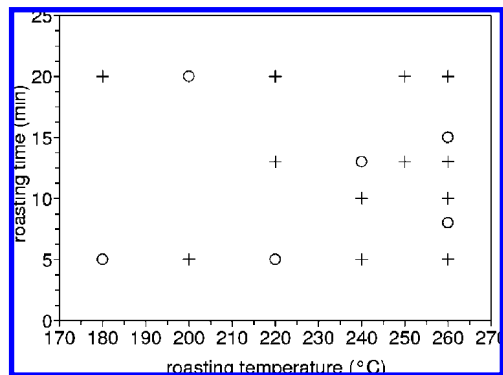
Figure 2. Experimental design used for obtaining data to build the models as well as data to validate the models. Key: +, data fed to the model; ○, data for model validation.

100% acetonitrile; this solvent was further maintained for 15 min. The total flow rate was 1.5 mL min⁻¹. The analytical column was placed in an oven (Waters Column Heater Module connected to a Waters Temperature Control Module, Waters, Guyancourt, France), and its temperature was regulated at 35 °C, enabling stability of the retention times. Detection was performed at selected excitation and emission wavelengths, programmed as follows: 0−9.6 min, 220/340 nm; 9.6−16.5 min, 230/410 nm; 16.5−20.0 min, 280/380 nm; 20.0−27.3 min, 250/420 nm; and 27.3−40.0 min, 286/420 nm. External calibration was performed using standard solutions of PAHs in THF in the range 5−500 or 5−50 μg L⁻¹ depending on the PAH concentrations in the samples. Identification of PAHs was based on peak retention times, by comparison with standards analyzed daily. Confirmation of the presence of suspected PAHs in coffee samples was achieved using HPLC coupled with a diode array UV−visible detector (HPLC-DAD) as well as gas chromatography coupled to mass spectrometry (GC-MS) as already reported (6). Thus, besides retention times, both UV and MS² spectra were used for confirming the presence of PAHs in the samples, by comparing them with those of standards in the same solvent.

Modeling. PAH formation during roasting results from complex chemical mechanisms involving numerous components and reactions. The system is so complex that it is impossible to model each chemical reaction, especially as the experimental data are limited to the measurement of the final PAH content of coffee after roasting under controlled conditions (given time and temperature). Yet, kinetic parameters (such as overall kinetic rate constant k and apparent activation energy E_a) are essential for kinetic modeling of PAH formation during roasting and thus predicting coffee quality loss during this thermal process. So, we tested different models with a variable number of assumptions on the chemical phenomena, with a view to predict the system global behavior. For complex behavior, it is also possible to use black box models. So, two kinds of model were used and compared as follows: kinetic models and statistical models (neural networks). The numbers of parameters to adjust differed for the tested models, varying from three to nine for the kinetic models and from five to 13 for the neural networks. To have a predictive model, the number of parameters to adjust should be as low as possible.

Databases. The database consisted of 39 experiments of coffee roasting, under 18 different time and temperature conditions (including replications) as illustrated in **Figures 2** and **3**, and additional measurements for green coffee. To validate the models, experiments were divided in two sets, a learning database with 25 experiments to compute the model parameters and a validation database (14 experiments) to test the prediction ability of the models.

Kinetic Models Based on Arrhenius Law. Several kinetic models were tested. The kinetic models presented here were selected for their compromise between simplicity and good fitting of experimental data. In all of the kinetic models tested, we assumed that the kinetic parameters of each reaction followed the Arrhenius law. The simple models (models 1 and 2) admit analytical solutions as detailed further in the text, whereas the solution of the complex kinetic model (model 3) was numerically computed with the ODE (ordinary differential equations) toolbox provided by Scilab (http://www.scilab.org/ 2007,
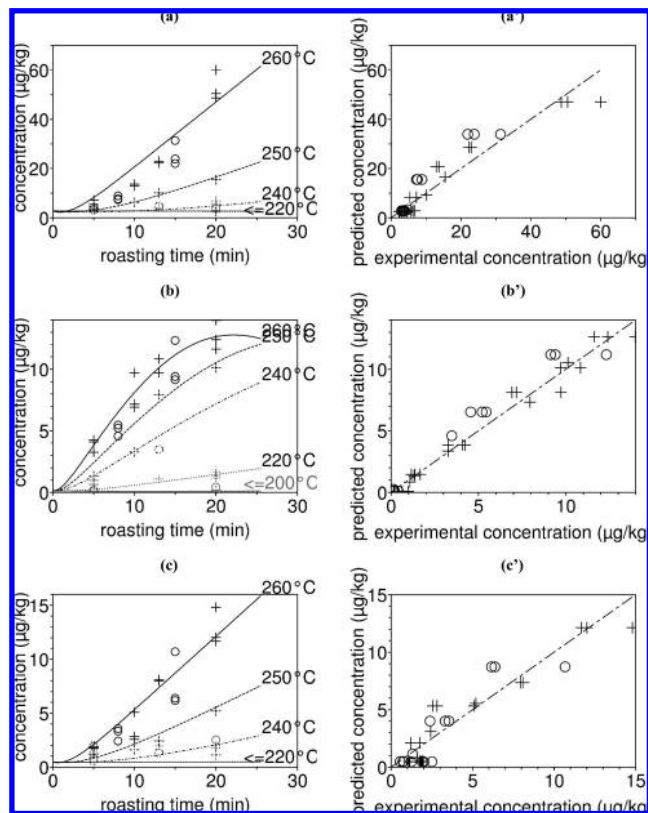
Figure 3. Comparison between experimental data profiles and simulated values given by the kinetic model 3 for pyrene, benz[*a*]anthracene, and chrysene during roasting under different conditions. (**a**−**c**) Response kinetics; (**a′**−**c′**) correlograms. (**a**, **a′**) Pyrene, $R^2 = 0.91$, $R_{valid}^2 = 0.80$; (**b**, **b′**) benz[*a*]anthracene, $R^2 = 0.98$, $R_{valid}^2 = 0.94$; and (**c**, **c′**) chrysene, $R^2 = 0.89$, $R_{valid}^2 = 0.81$. Key: −, model; +, data fed to the model; and ○, data for model validation.

April 20, version 4.1), containing the nonstiff predictor−corrector Adams method (*14*) and the stiff BDF (backward differentiation formula) method (*15*). The concentration values computed by these kinetic models were compared to the experimental estimated concentrations. All parameters of the models were adjusted by Levenberg−Marquardt optimization (*16*), using the datafit optimization routine of Scilab. The parameters were constrained to be realistic (i.e., positive kinetic reaction rate and energy of activation between 20 and 250 kJ mol⁻¹). The initial parameters were random values, and the optimization stopped when relative progress on the residue norm was smaller than 10^{-15}.

To avoid local optima, we repeated this optimization after changing random initial parameters from 300 times (for the complex kinetic model) to 30000 times (for the kinetic models with analytical solution). Therefore, we did a stochastic optimization. The optimized parameters leading to the best fit (best coefficient of determination) were selected. The prediction ability of the models was then tested on the validation database.

Neural Network Model. In the previous kinetic models, the shape of the kinetics was chosen *a priori* by the succession of the different reactions. Another way to model PAH concentrations as a function of time and temperature of the process was to use an empirical model. For process modeling, the ability of artificial neural networks (ANN) to integrate complex relationships between process parameters and product's quality was of great interest. Their major advantage was the ability of modeling without any assumption about the nature of underlying mechanisms.

ANNs are interconnected parallel systems consisting of simple processing elements, neurons. As in nature, the network function is determined largely by the connections between neurons, each connection having a weight coefficient attached to it. The neurons are grouped into distinct layers and interconnected according to a given architecture.

Table 3. Mean PAH Concentrations (with RSDs) and Toxic Equivalents (TEQ) in Green Coffee (*Arabica*) as Well as in Ground Coffee Roasted for Different Times Under 260 °C as the Inlet Air Temperature[a]

	0 min		5 min		8 min		10 min		13 min		15 min		20 min	
	concn (μg kg^{-1})	RSD (%)	concn (μg kg^{-1})	RSD (%)	concn (μg kg^{-1})	RSD (%)	concn (μg kg^{-1})	RSD (%)	concn (μg kg^{-1})	RSD (%)	concn (μg kg^{-1})	RSD (%)	concn (μg kg^{-1})	RSD (%)
Phen	8.89	9.72	8.39	17.14	12.83	5.15	13.32	6.26	13.53	10.37	12.21	7.90	17.37	5.26
Anthr	0.68	7.49	1.80	7.21	2.03	7.33	1.90	4.75	1.10	17.60	1.61	7.20	2.17	14.85
F	6.85	3.90	10.98	10.08	9.64	0.14	11.04	4.60	11.87	3.75	13.13	13.11	17.54	11.03
Pyr	3.27	15.14	6.60	15.83	7.94	10.30	13.16	3.42	22.0	5.08	25.74	19.30	53.05	11.47
B[a]A	0.20	41.52	3.86	13.80	5.08	9.09	7.93	19.58	9.57	14.04	10.29	17.18	12.67	9.42
Chrys	0.45	9.75	1.58	20.0	3.09	19.71	3.49	39.59	7.65	8.65	7.74	32.95	12.82	13.43
B[b]F	0.27	13.36	0.43	21.03	ND		ND		traces		traces		traces	
B[k]F	traces		0.17	14.85	traces		traces		traces		traces		ND	
B[a]P	traces		0.20	31.63	traces		traces		traces		traces		traces	
DB[ah]A	ND		0.37	31.65	ND		traces		ND		traces		ND	
B[ghi]P	ND		0.78	24.13	0.45	20.63	0.86	13.04	ND		1.02	50.99	1.71	36.49
Σ 11 PAHs	20.61		35.16		41.06		51.70		65.72		71.74		117.33	
TEQ (11 PAHs)	0.14		1.18		0.68		0.99		1.20		1.30		1.68	

[a] ND, not detected (no peak); traces, suspected presence of the compound (peak detected but with a signal to noise ratio below 3, meaning below the limit of detection).

In this study, a feed-forward, multilayer perceptron type of ANN was considered for the prediction of individual PAH formation during coffee roasting (*17*).

For a given network structure, the learning stage consists of determining the weights (and biases) of the connections that allow the network to best represent the experimental data. Thus, the learning is defined as a procedure that consists in adjusting the coefficients (weights and biases) of a network, to minimize an error function between the network outputs for a given set of inputs and the experimental concentrations. The gradient of the error function can be easily computed by the classical back-propagation procedure (*18*). In this work, the Levenberg–Marquardt algorithm was used (*16*), and the ANN computations were done using FANN software (http://leenissen.dk/fann, January 13, 2006, version 1.2.0-1) with octave software (http://www.octave.org, February 21, 2006, version 2.9). The coefficient of determination (R^2) between the experimental values and the network predictions was used as a criterion of model adequacy.

RESULTS

Experimental Data for Coffee Roasted under Controlled Conditions. A first set of experimental data was acquired by roasting green coffee for different times under 260 °C as the inlet air temperature. These conditions were chosen as the elevated roasting temperature should favor the formation of PAHs, enabling one to study the possible effect of roasting time on PAH content of coffee. Results are presented in **Table 3**. First, it is interesting to note that phenanthrene, fluoranthene, and pyrene are the major PAHs found in green coffee, with concentrations ranging from 3.27 to 8.89 μg kg^{-1}. The more toxic compounds, especially PAHs with five or six aromatic rings (such as benzo[*a*]pyrene), are present only at trace levels in green beans. To estimate the toxic equivalent (TEQ) to the content of the 11 PAHs, the toxic equivalent factors (TEF) were used (see **Table 2**), meaning that instead of simply adding the individual concentration of each PAH, concentrations were balanced with the respective TEF of the considered PAHs to take into account the different toxicity of the compounds (*19*). Consequently, the toxic equivalent is low for green coffee (0.14 μg kg^{-1}). As roasting is performed, the content of some PAHs (especially pyrene) increased. Similarly, the toxic equivalent increased up to 1.68 μg kg^{-1} after roasting for 20 min. Indeed, a clear formation of 4-aromatic rings PAHs is observed, whose proportion greatly increased over time. Of great concern is the formation of benz[*a*]anthracene, due to its toxicity. Also, low levels of benzo[*g,h,i*]perylene were found in all roasted samples. As its content was near the estimated limit of detection (around 0.20 μg kg^{-1}), variability of measurements

Table 4. Coefficient of Determination (R^2) for Each PAH Relative to the Database Used To Build the Models[a]

	kinetic model 1		kinetic model 3	neural network model		
	case 2	case 3	four reactions	one neuron	two neurons	three neurons
PAHs	$p = 3$[b]	$p = 5$	$p = 9$	$p = 5$	$p = 9$	$p = 13$
Phen	0.76	0.26	0.67	0.66	0.89	**0.95**
Anthr	0.38	0.39	0.74	0.57	**0.93**	**0.96**
F	0.55	0.50	0.38	0.42	0.89	**0.95**
Pyr	0.77	0.90	**0.91**	**0.97**	**0.97**	**0.97**
B[a]A	**0.94**	**0.96**	**0.98**	**0.96**	**0.97**	**0.98**
Chrys	0.80	0.88	0.89	**0.91**	**0.93**	**0.94**
B[b]F	<0.1	0.40	<0.1	0.29	0.74	0.90
B[k]F	<0.1	0.29	0.06	0.25	0.81	0.90
B[a]P	<0.1	<0.1	0.04	0.26	0.78	**0.91**
DB[ah]A	<0.1	0.19	0.83	0.53	0.87	**0.93**
B[ghi]P	0.55	0.61	0.31	0.73	**0.92**	**0.94**

[a] Values >0.90 are indicated in bold characters. Note that the coefficient of determination R^2 is the proportion of variability in a data set that is accounted for by a statistical model. [b] p is the number of unknown parameters to be determined by the model.

is large. Nevertheless, it seems that its content slightly increases with roasting time.

With a view of testing models for predicting the formation of some PAHs during roasting, in addition to these previous data, a new set of experiments was then conducted especially by roasting coffee at lower temperatures. The obtained data are presented below, with the results of the different modeling.

Modeling Using Kinetic Models Based on Arrhenius Law. Models based on Arrhenius law are often used for semiempirical modeling of complex reactions, for example, in crackers browning (*20*) or stigmasterol pyrolysis (*21*). Such models suggest a dependence of the overall kinetic rate constant with temperature as illustrated below
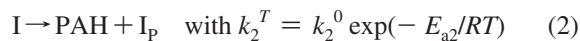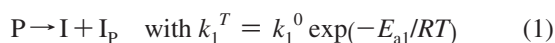
$$k^T = k^0 \exp(-E_a/RT)$$

where E_a is the apparent activation energy of the reaction (kJ mol^{-1}), R is the universal gas contant (0.0083145 kJ mol^{-1} K^{-1}), T is the temperature (K), k^T is the overall kinetic rate constant at temperature T, and k^0 is a pre-exponential constant (their units depend on the order of the reaction as detailed below). It is important to underline that both activation energy and pre-exponential constants are only apparent and do not refer to particular chemical reactions.

Table 5. Apparent Fitted Values for the Parameters of the Kinetic Models for Pyrene, Benz[a]anthracene, and Chrysene

kinetic parameters	units	pyrene	benz[a]anthracene	chrysene
$[PAH]_{t=0}{}^{a}$	$\mu g\ kg^{-1}$	2.79	0.15	0.46
	$mmol\ kg^{-1}$	13.8	0.66	2.03
		kinetic model 1—case 2		
$k_2{}^0$	$kg\ mol^{-1}\ min^{-1}$	model failed	1.47×10^6	model failed
E_{a2}	$kJ\ mol^{-1}$		77.4	
$[I]_{t=0}$	$mmol\ kg^{-1}$		50.6	
		kinetic model 1—case 3		
$k_1{}^0$	min^{-1}	1.4	5.5×10^8	model failed
E_{a1}	$kJ\ mol^{-1}$	20.8	92.6	
$k_2{}^0$	min^{-1}	5.67×10^3	3.60×10^3	
E_{a2}	$kJ\ mol^{-1}$	70.8	55.8	
$[P]_{t=0}$	$mmol\ kg^{-1}$	135	0.30	
		kinetic model 3		
$K_1 = k_1'{}^0 [R_1'][R_2']$	$mol\ kg^{-1}\ min^{-1}$	1.10×10^{-47}	9.78×10^{-48}	9.78×10^{-48}
$E_{a1'}$	$kJ\ mol^{-1}$	232	114	239
$K_2 = k_2'{}^0 [R_3']$	min^{-1}	0.685	4.49×10^{-4}	3.54×10^{-3}
$E_{a2'}$	$kJ\ mol^{-1}$	203	249	99.5
$K_3 = k_3'{}^0$	$kg\ mol^{-1}\ min^{-1}$	3.51×10^5	1.34×10^{10}	1.97×10^7
$E_{a3'}$	$kJ\ mol^{-1}$	131	33.3	155
$K_4 = k_4'{}^0 [R_5']$	min^{-1}	1.60×10^4	34.3	2.86×10^3
$E_{a4'}$	$kJ\ mol^{-1}$	249	72.3	197
$[P]_{t=0}$	$mmol\ kg^{-1}$	1.99	1.74	1.77

[a] $[PAH]_{t=0}$: These values were taken as the median values based on three analyses of green coffee samples.

Model 1. The first proposed model is very simple, based on two unimolecular successive reactions as indicated below

$$P \rightarrow I + I_P \quad \text{with } k_1{}^T = k_1{}^0 \exp(-E_{a1}/RT) \quad (1)$$

$$I \rightarrow PAH + I_P \quad \text{with } k_2{}^T = k_2{}^0 \exp(-E_{a2}/RT) \quad (2)$$

with P being the precursor, I an intermediate compound, I_P inactive reaction products, and $k_1{}^T$ and $k_2{}^T$ the overall kinetic rate constants of the first and second reactions, respectively, at temperature T.

As this simple model has been proposed to model the pyrolysis of stigmasterol, we may assume that P would be stigmasterol (a steroid present in green coffee), and I would be highly substituted aliphatic ring compounds (*21*). Several assumptions can be made on the respective rates of the two reactions of this kinetic model, as presented below.

Case 1: Reaction 2 Is Limiting, With Order One. First, we assumed that reaction 1 can be considered as fast, so that the limiting step is reaction 2, with apparent order one. Hence, the formation of PAH is driven by the following relation

$$d[PAH]_t/dt = k_2{}^T[I]_t = k_2{}^T([I]_{t=0} + [PAH]_{t=0} - [PAH]_t)$$

$$\text{with } k_2{}^T \text{ expressed in } min^{-1}$$

where t is the time (expressed in min), $[I]_t$ is the concentration of I at time t (expressed in mol kg^{-1}), $[PAH]_t$ is the concentration of the considered PAH at time t (expressed in mol kg^{-1}), and $[PAH]_{t=0}$ is the concentration of the considered PAH at time zero (expressed in mol kg^{-1}).

The exact solution of the above differential equation is

$$[PAH]_t = [PAH]_{t=0} + [I]_{t=0}[1 - \exp(k_2{}^T t)]$$

A total of three parameters (i.e., $[I]_{t=0}$, E_{a2}, and $k_2{}^0$, according to reaction 2) need to be estimated during the optimization of this model. To build the model, the value of $[PAH]_{t=0}$ was set to the median of estimated concentrations obtained from three experimental analysis of green coffee samples. Unfortunately, this model was not effective for most of the PAHs, especially

those which potentially contribute to the toxic equivalent in roasted coffee (best results obtained with benz[a]anthracene: $R^2 = 0.88$). Consequently, this case was left out.

Case 2: Reaction 2 Is Limiting, With Order Two. In this model, we assumed that reaction 1 can be still considered as fast, so that the limiting step is again reaction 2, but this time with an apparent order two. The formation of PAH can be expressed as follows:

$$d[PAH]/dt = k_2{}^T[I]_t{}^2 = k_2{}^T([I]_{t=0} + [PAH]_{t=0} - [PAH]_t)^2$$

$$\text{with } k_2{}^T \text{ expressed in } kg\ mol^{-1}\ min^{-1}$$

The solution of this differential equation is

$$1/([PAH]_t - [PAH]_{t=0}) = 1/[I]_{t=0} + 1/(k_2{}^T t[I]_{t=0}{}^2)$$

Again, a total of three parameters (i.e., $[I]_{t=0}$, E_{a2}, and $k_2{}^0$) need to be estimated during the optimization of this model. In the model, the value of $[PAH]_{t=0}$ was set to the median of data from three experimental analyses of green coffee samples as in the previous model. As shown in **Table 4**, benz[a]anthracene was the only compound for which this model was satisfactory ($R^2 = 0.94$), with an excellent ability to predict the validation database ($R_{valid}{}^2 = 0.93$). As the measurement error on experimental data is non-negligible and is taken into account in the computation of the coefficient of determination (residual error), this agreement can be considered as very good. The calculated apparent parameters are given in **Table 5**. However, the behavior of other PAHs suggests more complex apparent mechanisms.

Case 3: Reactions 1 and 2 Are Both Limiting, With Order One. Assuming both reactions are limiting with apparent first-order kinetics, the following relations can be written (with concentrations expressed in mol kg^{-1} and t being the roasting time expressed in min):

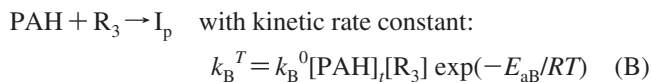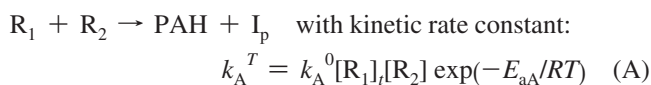$$[P]_t = [P]_{t=0} \exp(-k_1{}^T t) \quad \text{with } k_1{}^T \text{ expressed in } min^{-1}$$

$$[I]_t = [P]_{t=0} [\exp(-k_2{}^T t) - \exp(-k_1{}^T t)]k_1{}^T/(k_1{}^T - k_2{}^T)$$

$$\text{with } k_2{}^T \text{ expressed in } min^{-1}$$

Formation of Some PAHs during Coffee Roasting

J. Agric. Food Chem., Vol. 56, No. 10, 2008 **3653**

$$[PAH]_t = [PAH]_{t=0} + [P]_{t=0}\{k_2{}^T[1 - \exp(-k_1{}^T t)] -$$
$$k_1{}^T[1 - \exp(-k_2{}^T t)]\}/(k_2{}^T - k_1{}^T)$$

Considering that two unknown parameters must be determined for each overall kinetic rate constant (the apparent activation energy and the pre-exponential constant, according to reactions 1 and 2), this means that a total of five parameters need to be estimated during the optimization of this model ($[P]_{t=0}$, E_{a1}, $k_1{}^0$, E_{a2}, and $k_2{}^0$). The value of $[PAH]_{t=0}$ was set to the median of data from three experimental analyses of green coffee samples as already shown.

As shown in **Table 4**, this model was quite efficient in predicting the behavior of benz[*a*]anthracene ($R^2 = 0.96$) and still satisfactory for pyrene ($R^2 = 0.90$). The calculated parameters are presented in **Table 5**. Similar activation energies are observed, whereas reaction 1 is more rapid in the case of benz[*a*]anthracene. Validation of the model shows good agreement between experimental and simulated values, both for pyrene ($R_{valid}{}^2 = 0.89$) and benz[*a*]anthracene ($R_{valid}{}^2 = 0.94$). As the measurement error on experimental data is non-negligible and is taken into account in the computation of the coefficient of determination (residual error), this agreement can be considered as very good. Indeed, this simple model is quite predictive because it has a limited number of adjusted parameters (i.e., five). Unfortunately, this model was not effective for the others PAHs, which potentially contribute to the toxic equivalent in roasted coffee. Consequently, for the other components, more complex models describing more complex sets of reactions are required.

Model 2. For better modeling PAH behavior, we proposed another simple model, this time considering bimolecular reactions, which are preferentially expected under atmospheric pressure rather than unimolecular reactions (the latter usually occur under vacuum). In the considered model, PAH formation is followed by its subsequent degradation (as low molecular PAHs may be initially formed and then further degraded to higher molecular PAHs) as shown in the following consecutive reactions:
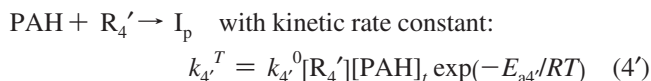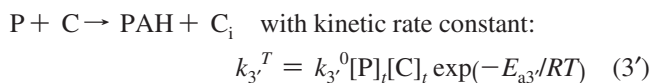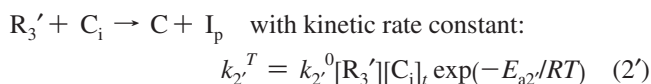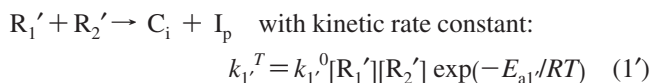
$$R_1 + R_2 \rightarrow PAH + I_p \quad \text{with kinetic rate constant:}$$
$$k_A{}^T = k_A{}^0[R_1]_t[R_2] \exp(-E_{aA}/RT) \quad (A)$$

$$PAH + R_3 \rightarrow I_p \quad \text{with kinetic rate constant:}$$
$$k_B{}^T = k_B{}^0[PAH]_t[R_3] \exp(-E_{aB}/RT) \quad (B)$$

with I_p being inactive products, R_2 and R_3 assumed to be in excess, and concentrations $[R_1]_t$ and $[PAH]_t$ (mol kg^{-1}) depending on time. Upon integration, this leads to the following relations, with $K_A = k_A{}^0[R_2]$ and $K_B = k_B{}^0[R_3]$:

$$[R_1]_t = [R_1]_{t=0} \exp[-K_A \exp(-E_{aA}/RT)t]$$

$$[PAH]_t = [PAH]_{t=0} + K_A[R_1]_{t=0} \exp(-E_{aA}/RT)$$
$$\{\exp[-K_A \exp(-E_{aA}/RT)t] - \exp[-K_B\exp(-E_{aB}/RT)t]\}/$$
$$[K_B \exp(-E_{aB}/RT) - K_A \exp(-E_{aA}/RT)]$$

The experimental data for some estimated PAH concentrations clearly express the formation of a product followed by its subsequent degradation. Unfortunately, the constraints on $k_A{}^0$, $k_B{}^0$, E_{aA}, and E_{aB} were incompatible with the data, so this model was inappropriate whatever the PAH considered.

Model 3. As we noted a variable time shift between experimental data and above simulated kinetics, as well as a visual second-order progression, we assumed that PAH formation is more complex than previously proposed. So, we switched

to the following complex autocatalyzing kinetics (*22*), where reaction 4′ was added as a standard degradation reaction of order one:

$$R_1' + R_2' \rightarrow C_i + I_p \quad \text{with kinetic rate constant:}$$
$$k_{1'}{}^T = k_{1'}{}^0[R_1'][R_2'] \exp(-E_{a1}/RT) \quad (1')$$

$$R_3' + C_i \rightarrow C + I_p \quad \text{with kinetic rate constant:}$$
$$k_{2'}{}^T = k_{2'}{}^0[R_3'][C_i]_t \exp(-E_{a2}/RT) \quad (2')$$

$$P + C \rightarrow PAH + C_i \quad \text{with kinetic rate constant:}$$
$$k_{3'}{}^T = k_{3'}{}^0[P]_t[C]_t \exp(-E_{a3}/RT) \quad (3')$$

$$PAH + R_4' \rightarrow I_p \quad \text{with kinetic rate constant:}$$
$$k_{4'}{}^T = k_{4'}{}^0[R_4'][PAH]_t \exp(-E_{a4}/RT) \quad (4')$$

with C an unknown reactive compound (either a free radical, a cation, or a catalyzer), C_i a form of this compound with lower reactivity, and R_1', R_2', R_3', and R_4' reactives.

In such a kinetic model, reaction 1′ is the initiation step of an autocatalytic production of the PAH molecule, reactions 2′ and 3′ are the propagation reactions, and reaction 4′ is the further degradation of PAH. Concentrations $[C_i]_t$, $[P]_t$, $[C]_t$, and $[PAH]_t$ (mol kg^{-1}) depend on time, while $[R_1']$, $[R_2']$, $[R_3']$, and $[R_4']$ (mol kg^{-1}) are supposed to be in excess and hence do not depend on time. For each PAH considered, nine parameters need to be optimized: the initial concentration $[P]_{t=0}$, the kinetic constants $K_{1'} = k_{1'}{}^0[R_1'][R_2']$, $K_{2'} = k_{2'}{}^0[R_3']$, $K_{3'} = k_{3'}{}^0$, $K_{4'} = k_{4'}{}^0[R_4']$, and the activation energies $E_{a1'}$, $E_{a2'}$, $E_{a3'}$, and $E_{a4'}$. The initial concentrations $[C_i]_{t=0}$ and $[C]_{t=0}$ are supposed to be negligible (the absence of these compounds at time zero or presence at low levels). As for previously tested kinetic models, the value of $[PAH]_{t=0}$ was set to the median of data from three experimental analyses of green coffee samples.

The model performed rather well to simulate the formation of pyrene, benz[*a*]anthracene, and chrysene as shown in **Table 4** and **Figure 3**. The kinetic parameters of this model, obtained for each compound by regression of the experimental data, are presented in **Table 5**. Of particular interest are the apparent activation energy values for PAH formation: 131, 33.3, and 155 kJ mol^{-1} for pyrene, benz[*a*]anthracene, and chrysene, respectively. These values are lower than the apparent activation energy values for PAH degradation, 249, 72.3, and 197 kJ mol^{-1}, so that formation is favored for low temperatures.

Modeling Using an ANN. A recent study reports possible prediction of PAH formation in premixed *n*-heptane flames using such models (*23*). So, this model was expected to be efficient in predicting the formation of some PAHs during coffee roasting. In practice, neural networks are recognized as good tools for dynamic modeling, with a major advantage of modeling without any assumption about the nature of underlying mechanisms.
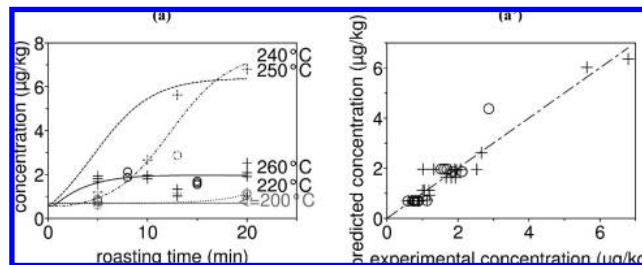
The parameters of the neural networks models were computed on the learning database and then tested on the validation database. In practice, to have a reliable model that can be used for prediction, the number of experiments must be greater than the number of parameters to compute. In our study, a neural network with three neurons in the hidden layer is at the limit of validity (13 parameters to determine), while two and one neuron(s) in the hidden layer are acceptable (only nine and five parameters, respectively). Consequently, we tested three neural networks with one hidden layer (with one, two, or three neurons in that layer).

Table 4 shows the efficiency of neural networks for different architectures. For some PAHs (namely, pyrene, benz[*a*]an-
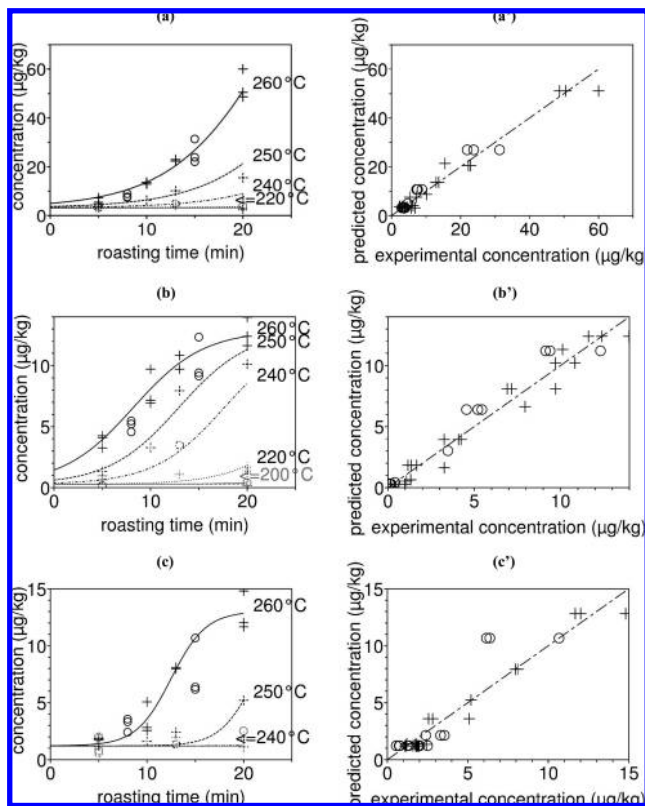
Figure 4. Comparison between experimental data profiles and simulated values given by the neural network (one neuron in hidden layer) for three PAHs during roasting under different conditions. (**a**–**c**) Response kinetics; (**a′**–**c′**) correlograms. (**a**, **a′**) Pyrene, $R^2 = 0.97$, $R_{valid}^2 = 0.93$; (**b**, **b′**) benz[*a*]anthracene, $R^2 = 0.96$, $R_{valid}^2 = 0.95$; and (**c**, **c′**) chrysene, $R^2 = 0.91$, $R_{valid}^2 = 0.78$. Key: −, model; +, data fed to the model; and ○, data for model validation.

Figure 5. Comparison between experimental data profiles and predicted values given by the neural network (two neurons in hidden layer) for anthracene during roasting under different conditions ($R^2 = 0.93$, $R_{valid}^2 = 0.84$). (**a**) Response kinetics and (**a′**) correlogram. Key: −, model; +, data fed to the model; and ○, data for model validation.

DISCUSSION

Our results provide further insight in the formation of PAHs during controlled roasting conditions. Satisfactory prediction could be obtained using kinetic models based on apparent reaction schemes or an artificial neuron network for some compounds, especially pyrene, benz[*a*]anthracene, and chrysene. The formation is very low for a wide range of temperatures and times and then rapidly increases at inlet air temperatures above 220 °C. In some cases, as observed for anthracene, the response curves show that the amount of this PAH grows with temperature until 250 °C and then drops. So, low molecular weight PAHs appear to be degraded at high temperatures into other components, probably high molecular weight PAHs.

However, as the presented kinetic models are based on apparent reaction schemes, we are unable to identify the real underlying mechanisms. So, the reactions really implicated in the formation of these contaminants remain unknown and need further investigation. Green coffee is a very complex matrix, and different reaction pathways are likely to occur during the roasting process. Roasting of some possible precursors under controlled conditions would probably help in understanding the chemical reactions responsible for PAH formation. Several coffee constituents may be considered as possible precursors of PAHs. Hence, the heating at 250 °C of trigonelline (*N*-methylpyridinium-3-carboxylate), a natural component of green coffee beans, leads to mutagenic compounds, with probably heterocyclic amines as well as mutagens of other types that could be PAHs (*24*). Similarly, lipids present in green coffee beans may be degraded into PAHs under roasting conditions, as PAHs (including the carcinogenic benz[*a*]anthracene, benzo[*a*]pyrene, and dibenz[*a,h*]anthracene) have been recently reported in the smoke generated upon heating lipids for 2 h under 200 °C (*25*). Intramolecular cyclization mechanisms are suspected from unsaturated fatty acids (such as oleic acid, linoleic acid, and linolenic acid), while degradation to form low molecular weight compounds containing the benzene ring followed by Diels−Alder cycloaddition are suggested from saturated fatty acids (such as stearic acid).

The formation of PAHs from steroids present in coffee beans, such as stigmasterol, may also be considered, even though such formation has been reported only for fast (≤1 s) heating of steroids under elevated temperatures (550−800 °C) until now (*21, 26, 27*). Hence, the first-order rate constants for the formation of phenanthrene and anthracene from steroids at 650 °C under flow pyrolysis were 0.138 and 0.057 min^{-1}, respectively (*26*). This is also the case of chlorogenic acid, a polyphenol whose pyrolysis (1.4 s, 700−850 °C) led to the formation of several PAHs, among them pyrene, fluoranthene, phenanthrene, and anthracene,

thracene, and chrysene), the simplest model with only one neuron in a hidden layer can explain more than 90% of the data variability. Results are also good on the validation database (R_{valid}^2 between 0.78 for chrysene and 0.95 for benz-[*a*]anthracene). Such a result is very interesting considering the low levels of PAH concentrations analyzed and the associated experimental variability. Looking at the response curves for these three PAHs, it appears that they face a simple behavior over the experimental range covered, with a very low formation over a wide range of temperatures and times (see **Figure 4**). The neural network with two neurons in hidden layer was found more efficient than simple neural networks and kinetic models for other PAHs, especially anthracene ($R^2 = 0.93$ for learning database and 0.82 for validation database) as indicated in **Table 4**. The response curves show that the content of this PAH increases with temperature up to 250 °C and drops for higher temperatures (see **Figure 5**). With regards to the other PAHs under investigation, the model failed to correlate with the experimental data, probably due to the lower levels of these compounds and the associated high variability of the experiments. In that case, three neurons in the hidden layer were required to achieve satisfactory modeling. However, such a complex model affords a low reliability, as the number of parameters to adjust (i.e., 13) is quite the same as the number of different roasting conditions in the learning database (i.e., 18).

Formation of Some PAHs during Coffee Roasting

J. Agric. Food Chem., Vol. 56, No. 10, 2008 **3655**

with suspected conversion of smaller PAHs to larger PAHs at high temperatures (*28, 29*).

Our results suggest that the roaster inlet air temperature should be at maximum 240 °C for 15 min to avoid the formation of toxic PAHs. However, such limits on roasting temperature and time were predicted according to the models presented in this paper. To generalize the presented models and the above limits to coffee beans of different lots or coffee varieties, the inlet air temperature should be replaced by the coffee bean temperature in the models, which can be measured or computed by a physical model taking in account data on mean size, water content, and thermophysics properties of the beans (*30*). As such physical models do no more admit analytical solutions and require long computations, modeling beans temperature was not feasible in the same time as the selection of several kinetic models.

Finally, it must be pointed out that other toxic contaminants are likely to be formed during the roasting step, such as acrylamide (a suspected carcinogen and mutagen compound), for which formation and reduction occurred during coffee roasting (*31, 32*). Progressive formation was observed under 150 °C with time, while maximum levels of acrylamide were noted after 10 and 5 min under 200 and 225 °C, respectively (*33*). Further degradation of acrylamide was noted for prolonged roasting. A similar trend has been recently observed for 5-hydroxymethyl-2-furfural, a Maillard product, with a rapid formation and subsequent degradation during the roasting of coffee at 240 °C (*34*). Thus, ideally, one should choose roasting conditions affording the highest organoleptic quality of coffee, along with minimization of toxic compounds, such as PAHs or acrylamide. However, this latter point seems delicate to achieve as optimum roasting conditions differ considering either PAHs or acrylamide.

ACKNOWLEDGMENT

LITERATURE CITED

(1) Kuratsune, M.; Hueper, W. C. Polycyclic aromatic hydrocarbons in coffee soots. *J. Natl. Cancer Inst.* **1958**, *20*, 37–51.

(2) Fritz, W. Polycyclische aromatische hydrocarbons kohlenwasserstoffe in malzkaffee, gerste und malz. *Naturwissenschaften* **1966**, *53*, 132.

(3) Badolato, E. S. G.; Martins, M. S.; Aued-Pimentel, S.; Alaburda, J.; Kumagai, E. E.; Baptista, G. G.; Rosenthal, A. Sistematic study of benzo[a]pyrene in coffee samples. *J. Braz. Chem. Soc.* **2006**, *17*, 989–993.

(4) Kruijf, N.; Schouten, T.; Van der Stegen, G. H. D. Rapid determination of benzo[*a*]pyrene in roasted coffee and coffee brew by high-performance liquid chromatography with fluorescence detection. *J. Agric. Food Chem.* **1987**, *35*, 545–549.

(5) Houessou, J. K.; Benac, C.; Delteil, C.; Camel, V. Determination of polycyclic aromatic hydrocarbons in coffee brew using solid-phase extraction. *J. Agric. Food Chem.* **2005**, *53*, 871–879.

(6) Houessou, J. K.; Benac, C.; Delteil, C.; Camel, V. Investigation of sample treatment steps for the analysis of polycyclic aromatic hydrocarbons in ground coffee. *J. Agric. Food Chem.* **2006**, *54*, 7413–7421.

(7) Houessou, J. K.; Maloug, S.; Lévèque, A.-S.; Delteil, C.; Heyd, B.; Camel, V. Effect of roasting conditions on the polycyclic aromatic hydrocarbons content in ground *Arabica* coffee and coffee brew. *J. Agric. Food Chem.* **2007**, *55*, 9719–9726.

(8) Commission Regulation (EC) No. 1881/2006 of 19 December 2006 setting maximum levels for certain contaminants in foodstuffs. *Off. J. Eur. Union* **2006**, L364/5−L364/24.

(9) Albertini, S.; Friederich, U.; Schlatter, Ch.; Würgler, F. E. The influence of roasting procedure on the formation of mutagenic compounds in coffee. *Food Chem. Toxicol.* **1985**, *23*, 593–597.

(10) Camargo, M. C. R.; Toledo, M. C. F. Cha-mate e café como fontes de hidrocarbonetos policiclicos aromaticos (HPAs) na dieta da populaçao de campinas. *Cienc. Tecnol. Aliment.* **2002**, *22*, 49–53.

(11) Arya, M.; Jagan Mohan Rao, L. An impression of coffee carbohydrates. *Crit. Rev. Food Sci. Nutr.* **2007**, *47*, 51–67.

(12) IARC (International Agency for Research on Cancer). *IARC Monogr. Eval. Carcinog. Risks Hum.* **1997**, *51*.

(13) Schwartzberg, H. G. Evolution of Coffee Roasting; AIChE conference, Cincinnati, Ohio, Oct 30−Nov 4, 2005; published on CD ROM 2005 AIChE Annual Meeting, ISBN 0-8169-0996-2.

(14) Shampine, L. F.; Gordon, M. K. *Computer Solution of Ordinary Differential Equations: the Initial Value Problem*; W. H. Freeman: San Francisco, 1975.

(15) Shampine, L. F.; Reichelt, M. W. The MATLAB ODE Suite. *SIAM J. Sci. Comput.* **1997**, *18*, 1–22.

(16) Moré, J. J. In *Numerical Analysis*; Watson, G. A., Ed.; Lecture Notes in Mathematics 630; Springer Verlag: New York, 1977; p 105.

(17) Hernandez-Perez, J. A.; Garcia-Alvarado, M. A.; Trystram, G.; Heyd, B. Neural networks for the heat and mass transfer prediction during drying of cassava and mango. *Innovative Food Sci. Emerging Technol.* **2004**, *5*, 57–64.

(18) Demuth, H.; Beale, M. *Neural Network Toolbox for Matlab−User's Guide Version 3*; The MathWorks Inc.: Natrick, MA, 1998.

(19) Collins, J. F.; Brown, J. P.; Alexeeff, G. V.; Salmon, A. G. Potency equivalent factors for some polycyclic aromatic hydrocarbons and polycyclic aromatic hydrocarbon derivatives. *Regul. Toxicol. Pharmacol.* **1998**, *28*, 45–54.

(20) Broyart, B.; Trystram, G.; Duquennoy, A. Predicting colour kinetics during cracker baking. *J. Food Eng.* **1998**, *35*, 351–368.

(21) Shin, E.-J.; Nimlos, M. R.; Evans, R. J. The formation of aromatics from the gas-phase pyrolysis of stigmasterol: Kinetics. *Fuel* **2001**, *80*, 1681–1687.

(22) Pokorny, J.; Yanishlieva, N.; Gordon, M. *Antioxidants in Food: Practical Applications*; Woodhead Publishing: Cambridge, 2001.

(23) Inal, F. Artificial neural network predictions of polycyclic aromatic hydrocarbon formation in premixed *n*-heptane flames. *Fuel Process. Technol.* **2006**, *87*, 1031–1036.

(24) Wu, X.; Skog, K.; Jägerstad, M. Trigonelline, a naturally occurring constituent of green coffee beans behind the mutagenic activity of roasted coffee? *Mutat. Res.* **1997**, *391*, 171–177.

(25) Chen, B. H.; Chen, Y. C. Formation of polycyclic aromatic hydrocarbons in the smoke from heated model lipids and food lipids. *J. Agric. Food Chem.* **2001**, *49*, 5238–5243.

(26) Britt, P. F.; Buchanan, A. C.; Kidder, M. K.; Owens, C. V.; Ammann, J. R.; Skeen, J. T.; Luo, L. Mechanistic investigation into the formation of polycyclic aromatic hydrocarbons from the pyrolysis of plant steroids. *Fuel* **2001**, *80*, 1727–1746.

(27) Britt, P. F.; Buchanan, A. C.; Kidder, M. K.; Owens, C. V. Influence of steroid structure on the pyrolytic formation of polycyclic aromatic hydrocarbons. *J. Anal. Appl. Pyrolysis* **2003**, *66*, 71–95.

(28) McGrath, T.; Sharma, R.; Hajaligol, M. An experimental investigation into the formation of polycyclic aromatic hydrocarbons (PAH) from pyrolysis of biomass materials. *Fuel* **2001**, *80*, 1787–1797.

(29) Sharma, R.; Hajaligol, M. Effect of pyrolysis conditions on the formation of polycyclic aromatic hydrocarbons (PAHs) from polyphenolic compounds. *J. Anal. Appl. Pyrolysis* **2003**, *66*, 123–144.

(30) Heyd, B.; Broyart, B.; Hernandez, J. A.; Valdovinos-Tijerino, B.; Trystram, G. Physical model of heat and mass transfer in a spouted bed coffee roaster. *Drying Technol.* **2007**, *25*, 1–6.

(31) Lantz, I.; Ternité, R.; Wilkens, J.; Hoenicke, K.; Guenther, H.; van der Stegen, G. H. D. Studies on acrylamide levels in roasting,

3656   *J. Agric. Food Chem.,* Vol. 56, No. 10, 2008

Houessou et al.

storage and brewing of coffee. <u>*Mol. Nutr. Food Res*</u>. **2006**, *50*, 1039–1046.

(32) Summa, C. A.; de la Calle, B.; Brohee, M.; Stadler, R. H.; Anklam, E. Impact of roasting degree of coffee on the in vitro radical scavenging capacity and content of acrylamide. <u>*LWT—Food Sci. Technol*</u>. **2007**, *40*, 1849–1854.

(33) Senyuva, H. Z.; Gokmen, V. Study of acrylamide in coffee using an improved liquid chromatography mass spectrometry method: Investigation of colour changes and acrylamide

formation in coffee during roasting. <u>*Food Addit. Contam*</u>. **2005**, *22*, 214–220.

(34) Murkovic, M.; Bornik, M.-A. Formation of 5-hydroxymethyl-2-furfural (HMF) and 5-hydroxymethyl-2-furoic acid during roasting of coffee. <u>*Mol. Nutr. Food Res*</u>. **2007**, *51*, 390–394.